Research Article Vol. 3, No. 5 / 15 May 2020 / OSA Continuum 1274

Sequence-coded coherent laser ranging with high detection sensitivity

KEREN SHEMER,[1] GIL BASHAN,[1] H. HAGAI DIAMANDI,[1] YOSEF LONDON,[1] TZUR RAANAN,[1] YOCHAI ISRAELASHVILI,[1] ALON CHARNY,[1] ITZIK COHEN,[2] ARIK BERGMAN,[1,3] NADAV LEVANON,[2] AND AVI ZADOK[1,*]

[1] *Faculty of Engineering and Institute for Nano-Technology and Advanced Materials, Bar-Ilan University, Ramat-Gan 5290002, Israel*
[2] *School of Electrical Engineering, Faculty of Engineering, Tel-Aviv University, Ramat-Aviv, Tel-Aviv 6997801, Israel*
[3] *Photonics Initiative, Advanced Science Research Center, City University of New York, New York, New York 10031, USA*
[*] *Avinoam.Zadok@biu.ac.il*

Abstract: The compression of extended, coded sequences allows for laser ranging measurements with low peak power levels. Previous realizations of this approach were restricted by additive noise of direct, incoherent detection. In this work we bring together pulse sequence coding and optical coherent detection to achieve very high sensitivity. Collected sequences with an overall energy equivalent to only 800 photons are successfully compressed. The observed sensitivity agrees with analytic predictions. Compared with incoherent detection, measurement durations are reduced by four orders of magnitude. The protocol is suitable for laser ranging over tens of kilometers, depending on atmospheric conditions.

1. Introduction

Optical measurements of the distance to a target are used in many civilian and military applications. Laser range-finders form the basis of light-radars (lidars), which are the sensors of choice in many autonomous vehicles [1–3]. Lidars are also used in sensing of cloud and aerosol [4,5], measurements of temperature and density in the atmosphere [6], and satellite and lunar ranging [7–9]. Recent advances include integrated optical phased arrays for solid-state beam steering [10–13] and the employment of single photon detectors [14,15]. Most range-finders rely on the transmission of short, intense and isolated laser pulses and time-of-flight measurements of reflected echoes. However, the transmission of high-peak-power pulses restricts the choice of available laser sources and may be intercepted by an adversary.

Alternatively, distance can be measured by continuous transmission of frequency-swept or modulated waveforms [16–23]. Sequence coding has been widely employed in microwave-frequency radars [23], and the technique has also been carried over to fiber optics [24,25]. The entire energy of a carefully-designed, long sequence of pulses can be compressed into a short and intense "virtual pulse" by post-detection processing [23,26–27]. The instantaneous power of the transmitted waveform can be four orders of magnitude weaker than those of single-pulse range finders. Therefore, sequence-coding can be realized using simple direct modulation of low-cost semiconductor laser diodes.

Effective protocols for the compression of optical pulse sequences were proposed by Levanon [26] and demonstrated experimentally by our groups [26–28]. An optical carrier was intensity-modulated by a carefully constructed, binary sequence, and simple direct detection was used at the receiver end. Distances up to 1,100 meters were measured in free space. However, compression of weak reflected echoes was restricted by additive detector noise. Incoherent

#386816 https://doi.org/10.1364/OSAC.386816
Journal © 2020 Received 26 Dec 2019; revised 4 Mar 2020; accepted 27 Mar 2020; published 11 May 2020

OSA CONTINUUM

detection is insensitive to phase information and limits the choice of sequences that may be used. In addition, it might be susceptible to interference among reflections from multiple targets. These difficulties may be resolved using coherent detection. Coherent receivers are widely deployed in optical fiber communication networks [29], and low-cost, integrated modules are being developed for data-center communication. Coherent detection is also used in spaceborne gravitational wave detection missions [30,31], and in high-sensitivity optical fiber sensors and ranging measurements [32–36]. In a remarkable recent example, coherent detection of coded sequences was used in distributed acoustic sensing over fiber at hundreds of kHz rates [24].

In this work, we report a proof-of-concept laser reflectometry experiment which combines pulse sequence compression and coherent detection [37]. Interference of very weak signals with a local oscillator (LO) in a coherent receiver generates a larger photocurrent and overcomes additive noise sources. The receiver sensitivity is limited only by the shot noise associated with the LO power [29]. We experimentally demonstrate that successful sequence compression requires accumulated signal energy that is equivalent to only several hundred photons. Sequence compression was achieved when the average collected energy per code symbol was only 0.002 of the photon energy. Compared with our previous studies of sequence coding with incoherent, direct detection, the acquisition duration is reduced by four orders of magnitude. The system is suitable for ranging over tens of kilometers in free space, depending on atmospheric conditions, and for distributed optical fiber reflectometry [24,38–42]. Partial results were presented briefly in a recent conference [37].

2. Principle of operation

The instantaneous power of the transmitted signal is repeatedly modulated by a series of pulses with duration T:

$$P(t) = P_0 \sum_n a_n \mathrm{rect}[(t - nT)/T] \tag{1}$$

Here P_0 represents constant power in Watts, t stands for time, $\mathrm{rect}(t) = 1$ when $|t| \leq 0.5$ and equals zero elsewhere, and a_n, $n = 1 \ldots N$, are the elements of a unipolar, binary sequence. In this work we employ a Legendre sequence L_N [26,27]. Sequences of this type are available at lengths $N = 4k - 1$, where k is an integer and N is a prime. Element a_n in the sequence equals 1 if an integer l exists such that $l^2 \bmod N = n \bmod N$. If no such integer exists, then $a_n = 0$ instead [26,27]. The sequence is replayed every N bits.

The Legendre sequence is compressed through cross-correlation with a bipolar representation $\tilde{L}_N$ of elements $\tilde{a}_n$, where $\tilde{a}_n = 2a_n - 1$. The periodic cross-correlation between L_N and $\tilde{L}_N$ is perfect in the following sense: It assumes peak values of $(N + 1)/2 \approx N/2$ at offsets that are integer multiples of N, with sidelobes of exactly zero everywhere else. Hence, in the absence of noise, compression of Legendre sequences in ranging applications does not introduce false targets. However, noise in any real-world system would introduce non-zero ranging sidelobes.

Let us denote the temporally-averaged optical power of the collected signal at the receiver end as P_S, so that the instantaneous signal power equals $2P_S$ when $a_n = 1$ and zero when $a_n = 0$. The receiver consists of four balanced detectors, for phase and polarization diversity. The photo-current at the output of each module is proportional to the beating pattern between an LO field and a single polarization and quadrature component of the received signal field. Consider the in-phase quadrature component along one polarization first. We assume that shot noise associated with a sufficiently strong LO is the dominant noise mechanism. The signal-to-noise ratio (SNR) in the detection of a single logical '1' bit is $2\eta P_S \cos^2\theta \cos^2\varphi \,/\, (h\nu\Delta f)$, where $h\nu$ is the photon energy, η denotes the detectors internal efficiency, and $\Delta f \approx 1/T$ is the measurement bandwidth. The term $\cos\theta$ represents the projection between the Jones vectors of the signal and LO fields, and φ is the optical phase difference between the two field components.

OSA CONTINUUM

The signal is detected over an integer number of repetitions M of the coding sequence, each N bits-long. Only half of the $M\,N$ signal bits carry power, while noise accumulates over all the signal bits. The SNR following cross-correlation is given by:

$$\begin{aligned} SNR_{Corr} &= \frac{MN\eta P_S}{2h\nu\cdot\Delta f}\cos^2\theta\cos^2\varphi \approx \frac{\eta P_S MNT}{2h\nu}\cos^2\theta\cos^2\varphi \\ &= \frac{\eta P_S T_{Meas}}{2h\nu}\cos^2\theta\cos^2\varphi = \frac{\eta}{2}N_{Phot}\cos^2\theta\cos^2\varphi \end{aligned} \tag{2}$$

Here $T_{Meas} \equiv MNT$ represents the measurement acquisition duration, and $N_{Phot} \equiv P_S T_{Meas}/h\nu$ expresses the collected energy as an equivalent number of photons. Similar expressions can be obtained for the orthogonal phase quadrature component, and for both phase components of the orthogonal polarization. Since the polarization and the phase of collected echoes are arbitrary, all four output ports of the coherent receiver must be examined simultaneously. In this work, we consider the maximum signal among the four compressed sequence outputs. In the best-case scenario, in which the signal is fully aligned with one polarization and phase component, the SNR of the processed trace reaches a maximum of $\eta N_{Phot}/2$. In the worst-case scenario, when the signal is equally split among the four terms, the SNR is four times lower. A stronger signal may be achieved through root-mean-square addition of all four balanced detectors. However, the noise power would increase four-fold. Compared with the choice of maximum, joint processing would only degrade the SNR. In addition, nonlinear processing analysis (such as root-mean-square) of the four outputs may introduce mixing terms and interference in detection of multiple targets. The processing of a single output does require that the coherence time of the transmitter source exceeds the acquisition duration.

A practical metric for the quality of the processed trace is its peak-to-sidelobe ratio (PSLR): the power ratio between the compressed correlation peak and the highest noise-induced sidelobe. The PSLR scales with SNR_{Corr}, but the two metrics are not equal. The value of SNR_{Corr} represents the average power due to noise across all sidelobes, whereas the PSLR is a measure of the worst-case: it is determined by the side-lobe of the highest power. The ratio between PSLR and SNR_{Corr} therefore depends on the number of sidelobes under consideration. In a previous study [28], we examined the noise-induced sidelobes of compressed sequences using order-statistics analysis, and derived the probability density function for the power of the strongest among N sidelobes. We found that for $N = 4003$, the expectation value of power in the strongest noise-induced sidelobe is 15 times higher than the average sidelobe power [28]. The analysis therefore suggests that the PSLR following coherent detection would be 15 times worse than the SNR_{Corr} obtained above: between $\eta N_{Phot}/30$ and $\eta N_{Phot}/120$, depending on $\cos\theta$ and on $\cos\varphi$.

We arbitrarily set the criterion for successful compression as a PSLR of at least 10. This requirement corresponds to a minimum number of signal photons N_{Phot} between 300 and 1,200, depending on the projections of the polarization and phase components. The necessary number of photons in a practical system might be higher due to detector inefficiency and excess losses in the receiver hardware. Note that sensitivity is expressed in terms of the overall collected energy of the echo signal and does not depend on the acquisition duration or the collected optical power alone.

3. Experimental results

We demonstrated coherent detection and compression of encoded sequences in a proof of concept experiment over fiber. A schematic illustration of the setup is shown in Fig. 1. Light from a coherent fiber laser source (NKT, 1550 nm wavelength, 18 mW output power, 5 kHz linewidth) was split by a 90/10 fiber-optic coupler. The continuous wave at the 90% port of the coupler was used as an LO and connected to the appropriate port of a Kylia COH-28 coherent photo-receiver. The LO power should be sufficiently high to overcome the thermal noise of the photo-detectors,

OSA CONTINUUM

hence most of the laser output power was routed to the LO path. Light at the 10% branch passed through an electro-optic Mach-Zehnder amplitude modulator (MZM), driven by the output voltage of an arbitrary waveform generator. The instrument repeatedly generated a 4,003 bit-long Legendre sequence, with symbol duration of 1 ns. This symbol duration corresponds to a length scale of 30 cm in air or 20 cm over fiber. The voltage of the generator was adjusted so that the transmitted power for '0' code bits reached zero.

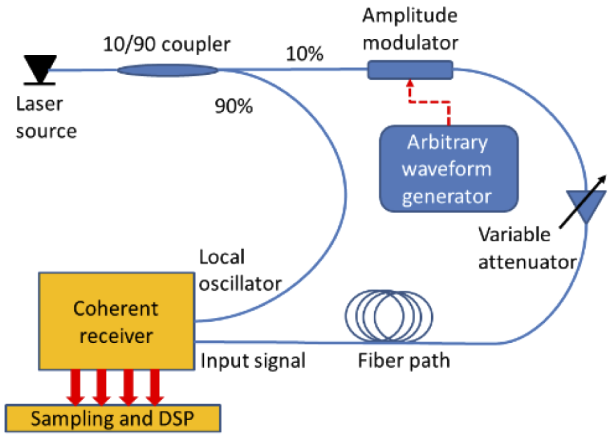

Fig. 1. Illustration of the setup used in a proof-of-concept experiment of the compression of coherently-detected coded sequences [37].

The MZM output waveform was connected to the input signal port of the coherent receiver through a manual variable fiber-optical attenuator (OPNETI MVOA, attenuation range between 0.6-60 dB). The input signal power P_S was measured for each acquisition using an optical spectrum analyzer. The outputs of the four detectors were sampled by a four-channel digitizing oscilloscope over different durations of T_{Meas}. The sampled traces were then correlated with a Legendre reference sequence through off-line digital signal processing, and the PSLR was calculated for each compressed trace. Figure 2 shows an example of a compressed waveform with $T_{Meas} = 400$ µs and $P_S = -92$ dBm. A clear peak is observed in the post-processed trace (presented arbitrarily at position $z = 0$). The PSLR of the processed signal replica is 14 dB, above the required minimum performance criterion.

Figure 3 shows the calculated PSLR as a function of P_S for the experimental data (solid lines, asterisk markers), alongside analytic predictions (dashed lines). Results are shown for different durations T_{Meas} (see legend for colors). Calculations are presented for the optimistic upper bound $\theta = \varphi = 0$. In the experimental data, each combination of P_S and T_{Meas} is represented by the best PSLR among the four receiver output ports as discussed above. The experimental results support the trends predicted by the analysis. The PSLR improves with signal power and with acquisition duration, as anticipated. Each level of PSLR is associated with constant collected signal energy $E_S = P_S T_{meas}$.

The minimum signal energy that is necessary to obtain a sufficient PSLR, or experimental sensitivity, is equivalent to 780 ± 100 photons. Analysis predicts an optimistic upper bound sensitivity of 430 photons. This sensitivity takes into consideration the specified detectors efficiency η of 90%, and 1 dB excess losses within the receiver hardware. The 2.4 dB sensitivity penalty in the experiment with respect to analysis is well within the 6 dB uncertainty associated with the state of polarization and relative phase of the signal. The optical power P_S of the weakest signal that could be compressed in the experiment with sufficient PSLR was -96 dBm. The measurement duration in that case was 400 µs.

OSA CONTINUUM

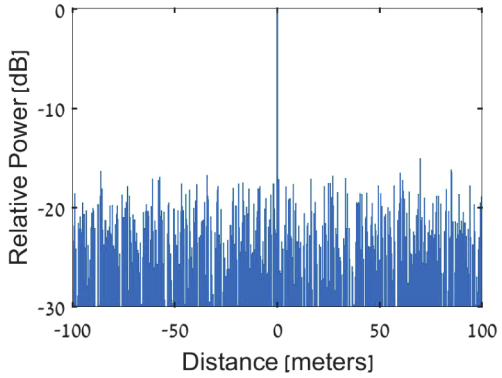

Fig. 2. An experimental signal trace following coherent detection and post-processing compression through cross-correlation with a reference sequence. The average optical power of the collected signal was -92 dBm, and the acquisition duration was 400 μs. The main peak represents the propagation delay between transmitter and receiver (positioned arbitrarily at $z = 0$). The power ratio between the peak and the highest noise-induced sidelobe (PSLR) is 14 dB.

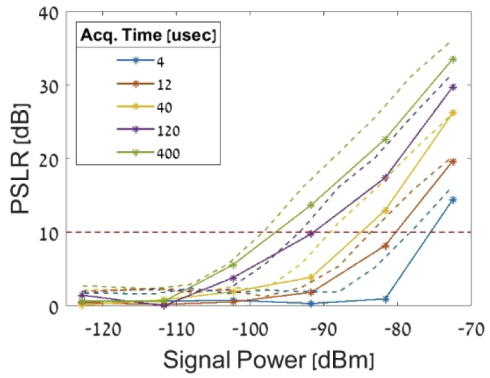

Fig. 3. Calculated power ratios between the compressed signal peak and the highest noise-induced sidelobe (PSLR), as a function of the signal power. Analytic predictions are shown in dashed lines. Experimental data is presented in solid lines and asterisk markers. Colors represent the acquisition duration (see legend). The threshold performance condition of PSLR = 10 dB is shown in a horizontal red dashed line.

Figure 4 presents four compressed waveforms, following propagation along different fiber lengths: an initial, arbitrary length and three additional increments of 19 cm, 47 cm and 66 cm. All measurements were taken with $T_{Meas} = 400$ μs and $P_S = -60$ dBm. The positions of compressed peaks correctly identify the changes in fiber length. The results are in qualitative agreement with the expectations. At poor SNR conditions, the ranging resolution may be estimated as $\frac{1}{2} v_g T$, where v_g denotes the group velocity. This estimate corresponds to 10 cm of fiber when $T = 1$ ns. Smaller range changes may be identified in high SNR conditions, such as those of Fig. 4.

Lastly, we examined the ranging resolution by the detection of two signal replicas that were added together. Light in the signal arm was split by a 50/50 coupler into two fiber paths of variable lengths. The two were recombined by a second 50/50 coupler at the coherent receiver input. Measurements emulated the simultaneous detection of two targets. Figure 5 shows four compressed waveforms, collected for paths lengths differences of 0 cm (a), 19 cm (b), 47 cm

OSA CONTINUUM

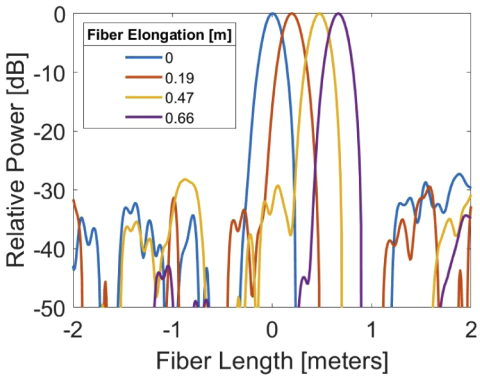

Fig. 4. Experimental signal traces following coherent detection and post-processing compression through cross-correlation with a reference sequence. The average signal power in all measurements was -60 dBm, and the acquisition duration was 400 µs. The waveforms were propagated over four different lengths of fiber (see legend). The positions of the compressed peaks correctly identify length changes.

(c), and 66 cm (d). All measurements were taken with $T_{Meas} = 400$ µs and $P_S = -36$ dBm. Two clear peaks with the expected distance separation may be identified in panels (c) and (d). The two peaks are barely distinguishable when the path difference was 19 cm in panel (b), and fully overlap in panel (a).

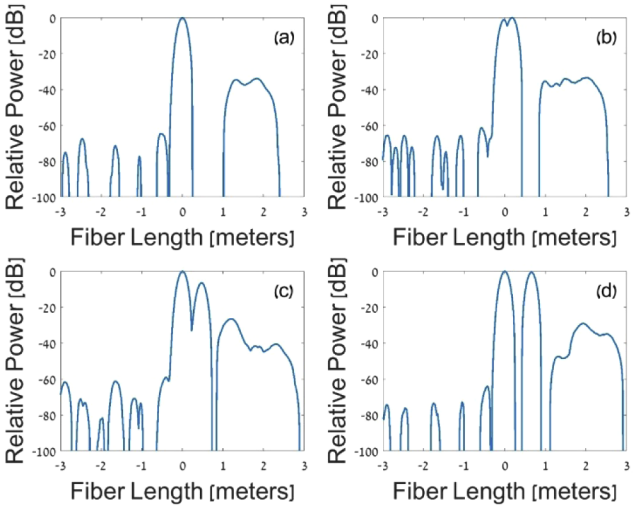

Fig. 5. Experimental signal traces following coherent detection and post-processing compression through cross-correlation with a reference sequence. The average optical power in all measurements was -36 dBm, and the acquisition duration was 400 µs. The signals were split in two fiber paths of variable length imbalance and recombined prior to detection. The paths lengths difference was 0 cm (a), 10 cm (b), 47 cm (c), and 66 (d). The two targets are clearly resolved in panels (c) and (d), but only barely resolved in panel (b).

OSA CONTINUUM

4. Conclusions

In this work, we demonstrated laser ranging measurements using sequence coding alongside coherent detection. Very weak replicas of transmitted signals were compressed and timed successfully. Analysis and experiments over fiber show that ranging can be obtained for a collected signal energy of only 800 photons. The weakest average power of coded signals that could be properly compressed in our previous studies using direct detection was -75 dBm. The required measurement duration at that power level was 200 ms. Here, signal replicas of the same power were successfully compressed with acquisition time of only 4 μs: an improvement by a factor of 50,000. Moreover, signals as weak as -96 dBm were successfully processed with a 400 μs-long acquisition duration. In the latter trace, the average collected energy per code bit was equivalent to only 0.002 of the photon energy. The spreading of transmitted energy over extended durations does not carry any penalty when realized with coherent detection. This property is in contrast with previous work using direct detection [28], where intense and short pulses provided higher SNR than extended sequences.

The analysis and experiments above relied on the compression of only one of the four polarization and quadrature components of the collected waveform echo: the one with the maximum signal. However, successful sequence compression based on a single component requires that the polarization and phase of the signal remain stable throughout the acquisition duration, reaching hundreds of micro-seconds. Atmospheric turbulence may induce phase fluctuations, which in turn would degrade the sensitivity of long-range measurements in free space. To work around this difficulty, root-mean-square addition of the four components may be carried out prior to the compression of the sequence. Such addition would retrieve the overall power of the collected signal, regardless of phase or polarization. As noted in Section 2 above, the processing of all four ports could degrade the PSLR by a factor of four, hence the selection of a single output port was preferred in this work. On the other hand, the compression of the combined signals from the four ports would be immune to any phase fluctuations slower than the nano-second durations of single symbols. Atmospheric turbulence also introduces temporary drops in the collected intensity [43].

The concept shows much promise for long-range measurements, potentially reaching tens of kilometers, depending on atmospheric conditions. Coherent receivers that are integrated on-chip are being rapidly developed towards data communications and may serve in low-cost range-finder systems. The high sensitivity of the proposed protocol is also useful for distributed optical time-domain reflectometry over fibers, with high spatial resolution and fast acquisition, and for high-rate distributed acoustic sensors [24,38–42]. Future work would explore applications in both free-space ranging and fiber reflectometry.

Acknowledgments

H. Hagai Diamandi is grateful to the Azrieli Foundation for the award of an Azrieli Fellowship.

Disclosures

The authors declare no conflicts of interest.

References

1. J. Hecht, "Lidar for self-driving Cars," Opt. Photonics News **29**(1), 26–33 (2018).
2. B. Schwarz, "LIDAR: Mapping the world in 3D," Nat. Photonics **4**(7), 429–430 (2010).
3. F. Rosique, P. J. Navarro, C. Fernández, and A. Padilla, "A systematic review of perception system and simulators for autonomous vehicles research," Sensors **19**(3), 648 (2019).
4. A. Ansmann, M. Riebesell, and C. Weitkamp, "Measurement of atmospheric aerosol extinction profiles with a Raman lidar," Opt. Lett. **15**(13), 746–748 (1990).
5. D. M. Winker, J. Pelon, J. A. Coakley, S. A. Ackerman, R. J. Charlson, P. R. Colarco, P. Flamant, Q. Fu, R. M. Hoff, C. Kittaka, T. L. Kubar, H. Le Treut, M. P. McCormick, G. Mégie, L. Poole, K. Powell, C. Trepte, M. A. Vaughan,

OSA CONTINUUM

and B. A. Wielicki, "The CALIPSO mission: a global 3D view of aerosols and clouds," Bull. Am. Meteorol. Soc. **91**(9), 1211–1230 (2010).
6. A. Hauchecorne and M. L. Chanin, "Density and temperature profiles obtained by lidar between 35 and 70 km," Geophys. Res. Lett. **7**(8), 565–568 (1980).
7. J. J. Degnan, "Millimeter accuracy satellite laser ranging: a review," Contributions of space geodesy to Geodyn. Technol. **25**, 133–162 (1993).
8. D. Arnold, O. Montenbruck, S. Hackel, and K. Sośnica, "Satellite laser ranging to low Earth orbiters: orbit and network validation," J. Geod. **93**(11), 2315–2334 (2019).
9. J. O. Dickey, P. L. Bender, J. E. Faller, X. X. Newhall, R. L. Ricklefs, J. G. Ries, P. J. Shelus, C. Veillet, A. L. Whipple, J. R. Wiant, J. G. Williams, and C. F. Yoder, "Lunar laser ranging: a continuing legacy of the Apollo program," Science **265**(5171), 482–490 (1994).
10. W. Xie, T. Komljenovic, J. Huang, M. Tran, M. Davenport, A. Torres, P. Pintus, and J. Bowers, "Heterogeneous silicon photonics sensing for autonomous cars [Invited]," Opt. Express **27**(3), 3642–3663 (2019).
11. Y. Zhang, Y. Ling, K. Zhang, C. Gentry, D. Sadighi, G. Whaley, J. Colosimo, P. Suni, and S. Ben Yoo, "Sub-wavelength-pitch silicon-photonic optical phased array for large field-of-regard coherent optical beam steering," Opt. Express **27**(3), 1929–1940 (2019).
12. C. Poulton, A. Yaacobi, D. Cole, M. Byrd, M. Raval, D. Vermeulen, and M. Watts, "Coherent solid-state LIDAR with silicon photonic optical phased arrays," Opt. Lett. **42**(20), 4091–4094 (2017).
13. S. A. Miller, C. T. Phare, Y.-C. Chang, X. Ji, O. A. Jimenez Gordillo, A. Mohanty, S. P. Roberts, M. C. Shin, B. Stern, M. Zadka, and M. Lipson, "512-element actively steered silicon phased array for low-power LIDAR," *2018 Conference on Lasers and Electro-Optics (CLEO)*, San Jose, CA, 2018, pp. 1–2.
14. L. Cohen, E. S. Matekole, Y. Sher, I. Istrati, H. S. Eisenberg, and J. P. Dowling, "Thresholded quantum LIDAR: exploiting photon-number-resolving detection," Phys. Rev. Lett. **123**(20), 203601 (2019).
15. A. Pawlikowska, A. Halimi, R. Lamb, and G. Buller, "Single-photon three-dimensional imaging at up to 10 kilometers range," Opt. Express **25**(10), 11919–11931 (2017).
16. R. Ula, Y. Noguchi, and K. Iiyama, "Three-dimensional object profiling using highly accurate FMCW optical ranging system," J. Lightwave Technol. **37**(15), 3826–3833 (2019).
17. J. Pastor-Graells, L. Cortés, M. Fernández-Ruiz, H. Martins, J. Azaña, S. Martin-Lopez, and M. Gonzalez-Herraez, "SNR enhancement in high-resolution phase-sensitive OTDR systems using chirped pulse amplification concepts," Opt. Lett. **42**(9), 1728–1731 (2017).
18. D. Arbel and A. Eyal, "Dynamic optical frequency domain reflectometry," Opt. Express **22**(8), 8823–8830 (2014).
19. P. Trocha, M. Karpov, D. Ganin, M. H. P. Pfeiffer, A. Kordts, S. Wolf, J. Krockenberger, P. Marin-Palomo, C. Weimann, S. Randel, W. Freude, T. J. Kippenberg, and C. Koos, "Ultrafast optical ranging using microresonator soliton frequency combs," Science **359**(6378), 887–891 (2018).
20. M.-G. Suh and K. J. Vahala, "Soliton microcomb range measurement," Science **359**(6378), 884–887 (2018).
21. W. Zou, S. Yang, X. Long, and J. Chen, "Optical pulse compression reflectometry: proposal and proof-of-concept experiment," Opt. Express **23**(1), 512–522 (2015).
22. J. Clement, C. Schnébelin, H. G. de Chatellus, and C. R. Fernández-Pousa, "Laser ranging using coherent pulse compression with frequency shifting loops," Opt. Express **27**(9), 12000–12010 (2019).
23. N. Levanon and E. Mozeson, *Radar Signals* (John Wiley & Sons, 2004).
24. J. J. Mompó, L. Shiloh, N. Arbel, N. Levanon, A. Loayssa, and A. Eyal, "Distributed dynamic strain sensing via perfect periodic coherent codes and a polarization diversity receiver," J. Lightwave Technol. **37**(18), 4597–4602 (2019).
25. Z. Wang, B. Zhang, J. Xiong, Y. Fu, S. Lin, J. Jiang, Y. Chen, Y. Wu, Q. Meng, and Y. Rao, "Distributed acoustic sensing based on pulse-coding phase-sensitive OTDR," IEEE Internet Things J. **6**(4), 6117–6124 (2019).
26. N. Levanon, "Noncoherent pulse compression," IEEE Trans. Aerosp. Electron. Syst. **42**(2), 756–765 (2006).
27. N. Levanon, I. Cohen, N. Arbel, and A. Zadok, "Non-coherent pulse compression-aperiodic and periodic waveforms," IET Radar Sonar Navig. **10**(1), 216–224 (2016).
28. N. Arbel, L. Hirschbrand, S. Weiss, N. Levanon, and A. Zadok, "Continuously operating laser range finder based on incoherent pulse compression: noise analysis and experiment," IEEE Photonics J. **8**(2), 1–11 (2016).
29. I. Kaminow, T. Li, and A. E. Willner, *Optical fiber telecommunications VB: systems and networks* (Elsevier, 2008).
30. J. W. Armstrong, F. B. Estabrook, and M. Tinto, "Time-delay interferometry for space-based gravitational wave searches," Astrophys. J. **527**(2), 814–826 (1999).
31. K. Danzmann, "LISA - an ESA cornerstone mission for a gravitational wave observatory," Class. Quantum Grav. **14**(6), 1399–1404 (1997).
32. L. B. Liokumovich, N. A. Ushakov, O. I. Kotov, M. A. Bisyarin, and A. H. Hartog, "Fundamentals of optical fiber sensing schemes based on coherent optical time domain reflectometry: signal model under static fiber conditions," J. Lightwave Technol. **33**(17), 3660–3671 (2015).
33. H. Iida, Y. Koshikiya, F. Ito, and K. Tanaka, "High-sensitivity coherent optical time domain reflectometry employing frequency-division multiplexing," J. Lightwave Technol. **30**(8), 1121–1126 (2012).
34. Y. Chen, K. M. Birnbaum, and H. Hemmati, "Active laser ranging over planetary distances with millimeter accuracy," Appl. Phys. Lett. **102**(24), 241107 (2013).

OSA CONTINUUM

35. R. Goldman, A. Agmon, and M. Nazarathy, "Direct detection and coherent optical time-domain reflectometry with Golay complementary codes," J. Lightwave Technol. **31**(13), 2207–2222 (2013).
36. J. Yang, B. Zhao, and B. Liu, "Coherent pulse-compression lidar based on 90-degree optical hybrid," Sensors **19**(20), 4570 (2019).
37. K. Shemer, G. Bashan, H. H. Diamandi, Y. Lodnon, A. Charny, T. Raanan, Y. Israelashvili, I. Cohen, N. Levanon, and A. Zadok, "Sequence-coded coherent laser range-finder with hundreds of photons sensitivity," in *Asia Communications and Photonics Conference (ACP)*, Chengdu, China Nov. 2019. OSA Technical Digest (Optical Society of America, 2019).
38. Y. Lu, T. Zhu, L. Chen, and X. Bao, "Distributed vibration sensor based on coherent detection of phase-OTDR," J. Lightwave Technol. **28**(22), 3243–3249 (2010).
39. D. Chen, Q. Liu, X. Fan, and Z. He, "Distributed fiber-optic acoustic sensor with enhanced response bandwidth and high signal-to-noise ratio," J. Lightwave Technol. **35**(10), 2037–2043 (2017).
40. H. Gabai and A. Eyal, "On the sensitivity of distributed acoustic sensing," Opt. Lett. **41**(24), 5648–5651 (2016).
41. M. R. Fernández-Ruiz, H. F. Martins, L. Costa, S. Martin-Lopez, and M. Gonzalez-Herraez, "Steady-sensitivity distributed acoustic sensors," J. Lightwave Technol. **36**(23), 5690–5696 (2018).
42. A. Bergman, T. Langer, and M. Tur, "Coding-enhanced ultrafast and distributed Brillouin dynamic gratings sensing using coherent detection," J. Lightwave Technol. **34**(24), 5593–5600 (2016).
43. A. Jurado-Navas, J. M. Garrido-Balsells, J. F. Paris, and A. Puerta-Notario, "A unifying statistical model for atmospheric optical scintillation," Chapter 8, *Numerical simulations of physical and engineering processes*, J. Awrejcewicz, ed. (InTech, 2011).